Structures 80 (2025) 109950

Contents lists available at ScienceDirect

Structures

journal homepage: www.elsevier.com/locate/structures

# Prediction of the compressive creep strain of the recombinant bamboo based on a variable-order fractional derivative defined Maxwell model

Sun Songsong *, Miao Zhiwei, Gong Xiaolin

*College of Automobile and Traffic Engineering, Nanjing Forestry University, Nanjing 210037, China*

ARTICLE INFO

*Keywords:*
Recombinant bamboo
Compressive creep
Variable-order Caputo fractional derivative model
Maxwell model

ABSTRACT

Natural fibre-reinforced composite materials, such as recombinant bamboo, usually exhibit obvious creep behaviour during the loading period. In previous studies, this property was usually examined through a standard creep experiment, which is time- and labour-consuming, particularly for long-term cases. In this study, an accelerated compressive creep experiment design method was introduced to shorten the time of the creep experiment process. First, several groups of standard compressive fracture experiments were conducted on the recombinant bamboo to determine the basic creep experimental parameters. Second, a short-term compressive creep experiment was conducted under several relatively high stress levels to record the strain evolution process. Then, a novel Maxwell viscoelastic model based on the theory of the modified Caputo fractional derivative was proposed for analysing the creep strain evolution process. Finally, the creep process of the specimen under other, lower stress levels was predicted based on the parameters obtained by fitting of the model to the experimental results obtained in the previous step and the evaluation of the effect of the stress level on the main parameters. The results showed that this approach can accurately predict the compressive creep strain growth process of a specimen, enabling the replacement of the actual experiment by model predictions, making this method suitable for wide use in industry.

## 1. Introduction

In recent years, recombinant bamboo has become one of the most commonly used natural fibre-reinforced composite materials [1]. Compared with similar materials made from wood or other natural resources, this material has several advantages, such as lower cost, better mechanical properties (particularly strength), and abundant resources, leading to its wide application in engineering practice. Consequently, accurate evaluation and determination of its main mechanical properties are necessary to guide the design and application of recombinant bamboo under the given conditions [2,3].

Several studies on this topic have been conducted in recent years. Huang et al.conducted an experiment on the double cantilever beam and end-notched beam models made of recombinant bamboo, based on which the main parameters of the material, such as the fracture toughness and damage mechanism, were determined, and the analytical expression for the fracture energy and flexibility equation of the specimen were derived [4,5]. Li et al.studied the tensile-compressive properties of recombinant bamboo in both parallel and vertical grain directions and proposed four types of mechanical constitutive relationship models that can accurately fit the stress−strain relationship [6]. Ma et al.investigated the bending fatigue properties of this material, and the results showed that the high-cycle fatigue life of the material may be more than $10^6$ under higher stress levels, and that the residual stiffness is influenced by the stress level [7]. Shangguan et al.examined the influence of the heat treatment technique on the material strength and concluded that the main effect can be attributed to the induration of the phenolic resin as well as the change in the crystallinity [8]. Yu et al. analysed the main factors that affect the strength of recombinant bamboo, such as the microstructure, the interface between the fibre and the matrix, and the manufacturing process, and discovered that increasing the compressive density during the manufacturing process and improving the interface quality can effectively enhance the strength [9]. Song et al.investigated the influence of both the fibre and matrix on the material strength and discovered that the fatigue life can be fitted accurately based on the two-parameter Weibull distribution function [10]. Yuan et al.analysed the hot oil bath technique and its influence on the strength of recombinant bamboo and discovered that only a

* Corresponding author.
*E-mail address:* 513194484@qq.com (S. Songsong).

https://doi.org/10.1016/j.istruc.2025.109950
Received 13 April 2025; Received in revised form 7 August 2025; Accepted 9 August 2025
Available online 15 August 2025

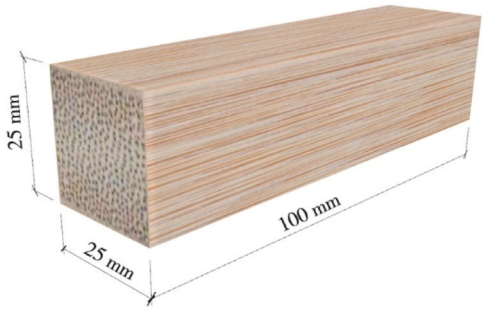


**Fig. 1.** Specimens used for the compressive experiment.

sufficiently long bath time will lead to an evident strength reduction due to the oil molecules adsorbed onto the interface of the fibre [11].

In previous studies on the mechanical properties of recombinant bamboo, the material was typically treated as an anisotropic elastic or plastic material. For fibre-reinforced adhesive materials, such as recombinant bamboo, obvious creep behaviour is usually observed under an applied load. In this field, Wei et al.and Chen et al.researched various types of creep behaviours of recombinant bamboo (tensile, compressive, and bending) based on the Burgers model, in which the relationship between the stress level and the amount of both viscous and viscoelastic creep can be determined accurately [12–15]. Liu et al.studied the creep properties of recombinant bamboo under different temperature conditions and discovered that the degree of viscous deformation within the whole deformation increased with temperature [16]. Liu et al.also conducted long-term creep prediction research based on accelerated creep tests under different temperature conditions, demonstrating that this method could shorten the time required for the creep experiment [17].

As introduced in the above-discussed reports, the creep experiment plays a vital role in the investigations of the creep properties of a material. This type of experiment can provide both detailed qualitative and quantitative analyses of the creep behaviour of a given material; however, the test period may last for days and months in long-term research, which may result in longer experimental time and high labour costs. In addition, according to experimental standards, the load amplitude during the creep experiment is typically determined according to the predefined load history. Therefore, any interruption or fluctuation in the load amplitude will disrupt the entire experimental process. This introduces additional risks and uncertainties into the experiment. Thus, determination of the creep properties of a material in a relatively short time and at a lower cost is important for applications.

To overcome this problem, a new accelerated creep experimental method was proposed in this study. First, a compressive creep experiment was conducted on a given specimen under a time-varying load at relatively high stress levels. Subsequently, a variable-order Caputo fractional derivative-defined Maxwell model was chosen to analyse the viscoelastic properties of the material and the effect of the stress level on the main model parameters. Finally, the model parameters under other stress levels can be easily determined based on the results obtained in the previous step. Thus, the compressive creep strain can be determined based on the model predictions. The results showed that this method can accurately predict the creep strain growth of recombinant bamboo under several stress levels, and is an effective approach for guiding the creep experiment design process in engineering applications.

## 2. Material and methods

### 2.1. Material

Currently, the combined pressing and gluing technique is the most widely applied method for the manufacturing of recombinant bamboo. During the first step of the manufacturing process, bamboo fibres were drawn from the raw material via the selected approach (defibreing, alkalisation, or other methods) and dried until the water content reaches the specified value. The dry fibres were then immersed in phenolic resin and mixed uniformly in the appropriate ratio. Finally, the mixture was placed in a steel box and compressed at high temperatures and pressures (usually no less than 7 MPa). Thus, the bamboo fibres recombined and adhered to each other with the help of phenolic resin, and a completely new kind of composite material was produced.

The recombinant bamboo used in this study was purchased from Taohua Jiang Company, Ltd. In addition, raw bamboo material was cut from four-to five-year-old Nanzhu bamboo plants in Hunan Province, China. The research objective of this study was to investigate the compressive creep behaviour of recombinant bamboo. Therefore, cuboid specimens were produced according to ASTMD 143–94; detailed information on the structural features and dimensions of the specimens is provided in Fig 1.

### 2.2. Creep strain prediction method

As introduced in the previous section, the main components of recombinant bamboo are bamboo fibres and phenolic resin. For these two types of materials, clear creep behaviour is usually observed during the loading period. Consequently, the recombinant bamboo itself also shows clear creep behaviour. The creep properties of the composite materials are usually determined through standard creep experiments. This approach can accurately evaluate the creep properties of a given material; however, the experiment is usually performed for hours or days, which may result in high time and labour costs. In addition, according to our previous study, the mechanical properties of recombinant bamboo usually exhibit clear variations among the samples, which means that the sample size of the experiment should be sufficiently large to guarantee the reliability of the experimental results.

Moreover, according to experimental standards, the load amplitude during the creep experiment process is usually determined according to the predefined load history. Therefore, any interruption or fluctuation in the load amplitude will disrupt the entire experimental process. This introduces additional risks and uncertainties into the experiment. Thus, determination of the creep properties of a material in a relatively short time and at a lower cost is important for applications. According to a previous study, when recombinant bamboo was under a static load, the stress level caused by the load affected its creep properties [13]. Accordingly, an accelerated creep experimental method can be proposed. The entire process is divided into three steps.

Step 1. In this step, a time-varying compressive load was applied to a specimen under relatively high stress levels to record short-term experimental data. In order to conduct further verification of the universality of the proposed method, in this paper there are four specimens in all. A viscoelastic constitutive model was then selected to analyse the strain evolution process.

Step 2. The main model parameters of the selected viscoelastic model and stress level were determined. The values of the model parameters under any other stress level can then be calculated based on the proposed relationship function.

Step 3. The creep strain of the same specimen under relatively lower stress levels and longer times was predicted based on the model parameters obtained in the previous step. Thus, the actual experimental process can be replaced by model predictions if prediction accuracy is sufficiently high.

### 2.3. Experimental method

As mentioned in the previous reports on the material creep, the stress amplitude during the test process is usually defined based on the related strength parameters of the material itself [14]. In this study, the creep behaviour was compressive. Therefore, it is necessary to determine the compressive strength of the material before starting the creep

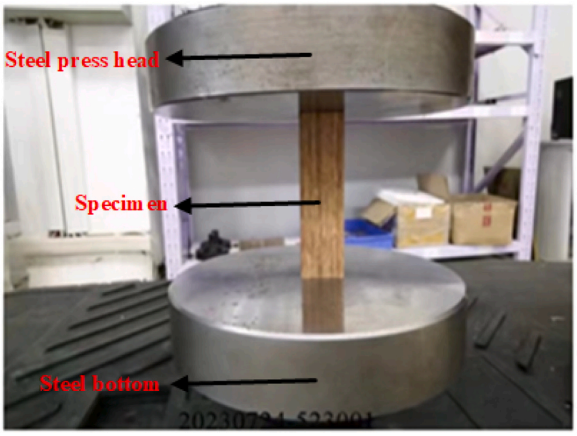


**Fig. 2.** Equipment and specimen for the compressive fracture experiment.

experiments. According to our previous study, this parameter can be determined through a combination of statistical analysis and the standard compressive fracture experiment [18]. Fig. 2 shows the equipment for this test. The specimen is placed vertically on the steel bottom, and a steel pressure head is used to press on the top of the specimen. During the experiment, the load amplitude was gradually increased until the specimen broke. This experiment was performed according to the GB T1041–2008 standard [19]. The equipment was controlled using a connected computer. In addition, the specimen was produced through the rotary-cut technique, and the length-width ratio of the specimen was also able to fulfil the demand of the standard, which can guarantee thealignment of the specimen in the compression machine. The entire compressive fracture experiment was carried out by the STANDARD Testing Group Co., Ltd. The temperature of the experiment is set to be 25 ℃, and the humidity is 40 %.

During the creep experiment, the creep strain generated by the applied load is a key parameter for monitoring the state of the specimen. However, according to a previous study, compared with the commonly used strain gauges, the extensometer is more suitable for measuring the strain during the creep experiment, particularly for compressive strain [20]. Fig. 3 shows the creep strain recording equipment, where the length of the extensometer used in this study was 50 mm. Consequently, the value of the strain can be indirectly recorded as

$$\varepsilon = \frac{\Delta L}{50} \tag{1}$$

where $\Delta L$is the offset variable of the extensometer. The creep experiment was performed according to the ASTM D2990–17 standard. The loading rate was 0.1 mm/min, and the whole equipment was controlled by the computer. The experiment was conducted with the UTM5504-GD microcomputer-controlled test equipment During the experiment, the sampling frequency was set to 1 $min^{-1}$. The condition of the creep test is set to be the same with that of the compressive fracture experiment.

According to the thermodynamics theory, a specimen made using the hot-pressing technique usually contains a residual stress field caused by the uneven temperature field generated during the manufacturing process, which may affect the creep strain experiment results. Fig. 4 presents a detailed load history for the pretreatment of the specimen carried out according to the experiment standard to release the residual stress and guarantee the reliability of the creep experiment results.

### 2.4. The statistical analysis method

According to previous research, a primary conclusion can be proposed that compared with metal and artificial composite materials, the recombinant bamboo exhibits more dispersion with regard to its static mechanical properties, which can be attributed to the diversity of natural fibers and manufacturing techniques [18]. Thus, the corresponding statistical analysis of the experimental data becomes necessary to determine the actual value of the strength at a given survival rate.

To today, there are three kinds of commonly used statistical analysis methods in this field, the normal distribution function, the lognormal distribution function and the three-parameter Weibull distribution function. For the normal distribution model, the expression of the probability density function is usually expressed as:

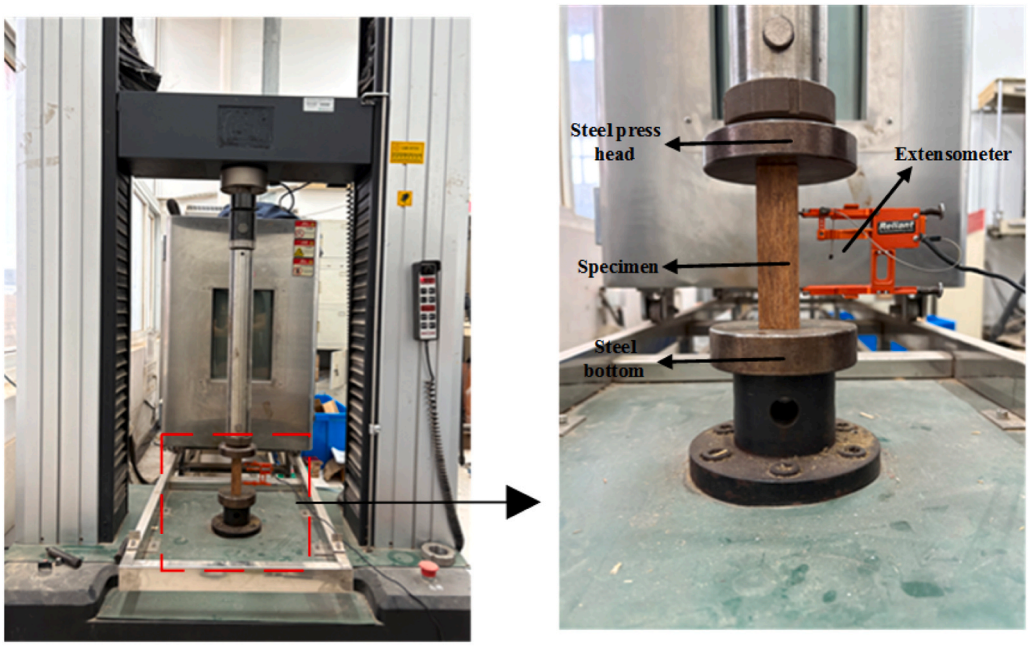


**Fig. 3.** Creep strain recording equipment: (a) the whole equipment, (b) the partial area of the specimen.

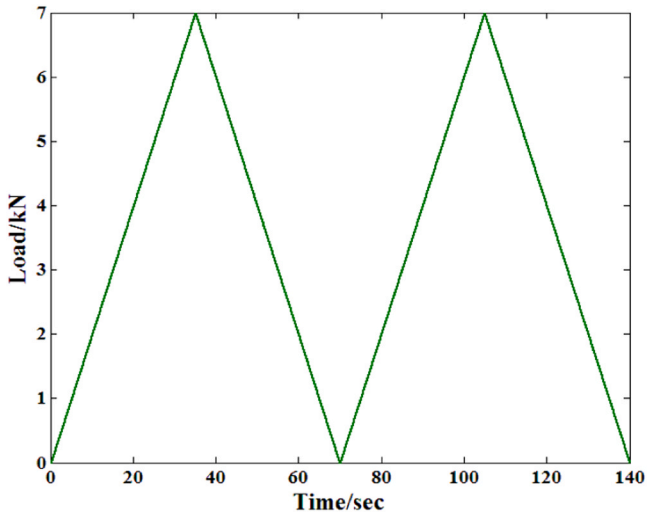


**Fig. 4.** Load history for the pretreatment process.

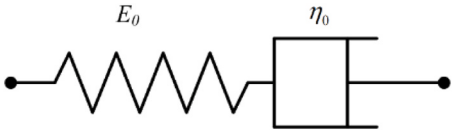


**Fig. 5.** The definition of the Maxwell model.

$$y = \frac{1}{\sqrt{2\pi}m}\exp\left(-\frac{(x-\mu)^2}{2}\right) \tag{2}$$

In this equation, $\mu$ is the mathematical expectation of the random variable, and $m$is the standard deviation of the random variable. Based on this definition, the fitting approach can be converted to the linear regression analysis by the following equations:

$$x_i = FS_i \tag{3}$$

$$y_i = \Phi^{-1}(F_i) \tag{4}$$

where $FS_i$ is the ith experimental result from the arrangement in the previous chapter, and$\Phi$ is the standard normal function, $y_i$ is the survival rate of the *ith* experiment result. According to previous study, the survival rate can be approximately defined by the media rank [18]. The definition of this parameter can be expressed as:

$$F_i = \frac{i_k - 0.3}{n + 0.4} \tag{5}$$

as shown in Eq. (4), $i_k$ is the failure number of the *ith* experimental result, $n$is the sample size. The linear equation can be determined by the minimum variance fitting method of the converted data. The expression of the equation is as follows:

$$y = \hat{a} + \hat{b}x \tag{6}$$

Based on this assumption, the mean and variance values according to the distribution function can be expressed as:

$$\hat{\mu} = -\frac{\hat{a}}{\hat{b}} \tag{7}$$

$$\hat{m} = \frac{1}{\hat{b}} \tag{8}$$

For the lognormal distribution model, the expression of the probability density function is usually expressed as:

$$y = \frac{1}{\sqrt{2\pi}m}\exp\left(-\frac{(\ln x - \mu)^2}{2}\right) \tag{9}$$

Based on this definition, a similar linear regression fitting approach can be conducted under this condition. The corresponding parameters can be expressed as:

$$x_i = \ln(FS_i) \tag{10}$$

$$y_i = \Phi^{-1}(F_i) \tag{11}$$

$$\hat{\mu} = \exp\left(-\frac{\hat{a}}{\hat{b}} + \frac{1}{2\hat{b}^2}\right) \tag{12}$$

$$\hat{m} = \sqrt{\exp\left(\frac{2\hat{a}}{\hat{b}} + \frac{1}{\hat{b}^2}\right)\left[\exp\left(\frac{1}{\hat{b}^2}\right) - 1\right]} \tag{13}$$

According to the definition, the three-parameter Weibull distribution function can be expressed as:

$$y = 1 - \exp\left[-\left(\frac{x-\gamma}{\eta}\right)^{\beta}\right] \tag{14}$$

where $\gamma$ is the location parameter, $\eta$ is the scale parameter and $\beta$ is the shape parameter.From this equation, a clear conclusion can be proposed that unlike that of the normal and lognormal models, the parameters in a three-parameter Weibull model cannot be calculated through the linear regression fitting approach. In previous studies, usually a Neld-Mead method was usually adopted for determining the parameters [21]. This approach first determines the location parameter $\gamma$ based on a searching optimization algorithm, among which the value of this parameter can be fixed by an iterative solution. In every iteration course, the relationships between these three parameters can be expressed as:

$$x_i = \ln(FS_i - \hat{r}_i) \tag{15}$$

$$y_i = \ln(-\ln(1 - F_i)) \tag{16}$$

where $\hat{r}_i$ is the given value of $\gamma$ in the ith iteration. This approach can determine the corresponding necessary parameters quickly and accurately. Based on this model, the mathematical expectation of the random variable and the standard deviation of random variable can be proposed as:

$$\hat{\mu} = \hat{\gamma} + \hat{\eta}\cdot\Gamma\left(\frac{1}{\hat{\beta}} + 1\right) \tag{17}$$

$$\hat{m} = \hat{\eta}\sqrt{\Gamma\left(\frac{2}{\hat{\beta}} + 1\right) - \Gamma\left(\frac{1}{\hat{\beta}} + 1\right)^2} \tag{18}$$

where $\Gamma$is the Gamma distribution function.

### 2.5. Variable-order fractional derivative theory defined Maxwell model

To realise the prediction method proposed in the previous Section 2.3 to predict the creep strain growth behaviour of recombinant bamboo, it is necessary to choose a suitable viscoelastic model to analyse the creep strain evolution process. Various types of mechanical constitutive models have been developed to investigate the response properties during the creep process based on specified parameters (such as stress, strain, and displacement). Among these, the Maxwell model is a classic model. The main components of the model are shown in Fig. 5 [18].

As shown in Fig. 5, the model is composed of two parts: a spring body

**Table 1**
Results of compressive fracture experiments on the recombinant bamboo.

| Serial number | Compressive load | Compressive strength |
|---|---|---|
| 1 | 56.1 KN | 89.76 MPa |
| 2 | 59.3 KN | 94.8 MPa |
| 3 | 52.6 KN | 84.18 MPa |
| 4 | 60.6 KN | 96.97 MPa |
| 5 | 54.4 KN | 87.1 MPa |
| 6 | 62.8 KN | 100.43 MPa |
| 7 | 61.4 KN | 98.2 MPa |
| 8 | 59.1 KN | 94.56 MPa |
| 9 | 60.8 KN | 97.28 MPa |
| 10 | 59.5 KN | 95.21 MPa |
| 11 | 58.6 KN | 93.8 MPa |

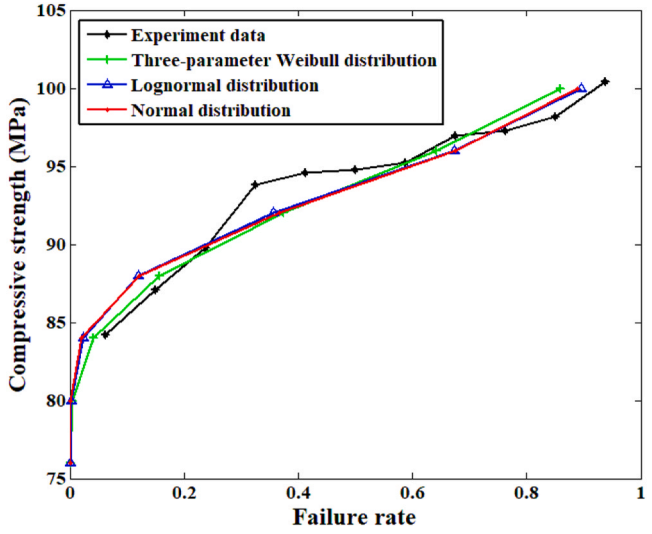


**Fig. 6.** Results of the statistical analysis of the compressive strength based on different models.

and an Abel dashpot body. In a previous study, the viscoelasticity of the model was determined using a fractionally defined dashpot body. The stress–strain relationship of the model based on the theory of fractional derivatives can be expressed as:

$$\sigma_1 = \sigma_2 = \sigma_0 \tag{19}$$

$$\sigma_1 = E_0\varepsilon_1(t) \tag{20}$$

$$\sigma_2 = \eta_0\frac{d^\alpha\varepsilon_2(t)}{dt^\alpha} \tag{21}$$

where $\sigma_0$is the total stress provided by the model; $\sigma_1$ and $\sigma_2$are the stresses of the spring body and Koeller dashpot body, respectively; $\varepsilon_1$ and $\varepsilon_2$ are the strains of the spring body and Koeller dashpot body, respectively; $E_0$ is the elastic modulus;$\alpha$is the order of the fractional derivative; and $\eta_0$ is the viscosity coefficient. To date, some commonly used fractional derivative models have been applied to analyse the creep behaviour of viscoelastic materials, among which the Caputo model is an effective tool. The model can be expressed as [22]:

$$D^\alpha f(t) = \int_0^t \frac{f'(\tau)}{\Gamma(1-\alpha)(t-\tau)^\alpha}d\tau \tag{22}$$

where $\Gamma$ is the Gamma function. Thus the stress-strain relationship of the dashpot body defined based on the Caputo fractional derivative approach can be expressed as:

$$\sigma(t) = \eta_0 D^\alpha\varepsilon(t) = \eta_0\int_0^t \frac{\varepsilon'(\tau)}{\Gamma(1-\alpha)(t-\tau)^\alpha}d\tau \tag{23}$$

According to our previous study, the order of the derivative model is influenced by the stress level. In this study, the load history was a time-varying factor. Consequently, the model exhibited a clear variation with time. The variable-order Caputo model is defined as

$$D^\alpha f(t) = \int_0^t \frac{f'(\tau)}{\Gamma(1-\alpha(\tau))(t-\tau)^{\alpha(\tau)}}d\tau \tag{24}$$

Based on this assumption, the stress–strain relationship provided by the variable-order Caputo model defined by the Koeller dashpot body can be determined. The detailed analysis process is shown in the appendix part.

In addition, among the main components of the Maxwell model, the spring body contains only one parameter, the elastic modulus, which can be easily determined according to the initial value of the strain at the beginning of the compressive creep experimental process.In this paper, the fitting of the experimental data could be performed by adjusting the value of the order and the coefficient of viscosity of the Abel dashpot body, where the values of these two parameters are considered as independent variables, and the response strain provided by the Maxwell model is the argument. The goal of the fitting approach is to minimise the relative differences between the experimental data and the response function provided by the Maxwell model. The fitting process is carried out via the Levenberg–Marquardt algorithm provided by MATLAB software.

## 3. Results and discussion

### 3.1. Compressive fracture experiment results

According to the method proposed in Section 2.2, the first step of the research process was to determine the compressive strength of the material to provide the basic load parameters for further creep experiments. According to our previous study, the mechanical parameters of recombinant bamboo show clear variation, necessitating the use of statistical analysis and a sufficiently large sample size [18]. Table 1 shows the detailed results of the compressive fracture experiments on the material for eleven experimental samples. Additionally, the coefficient of variation in this experiment was 5.2 %, which fulfilled the requirement of a variation no greater than 20 % [21].

Fig. 6 shows a statistical analysis of the experimental results obtained using the three selected models. According to our previous study, of these three commonly used statistical analysis methods for the mechanical experimental data of recombinant bamboo, the three-parameter Weibull model is the most suitable choice owing to its ability to provide a theoretical estimate of the safe time period. Based on this model, the compressive strength of the recombinant bamboo under 100 % survival rate can be determined as 75.8 MPa [23].

### 3.2. Short-term creep experiment results

According to the research method mentioned in the Methods section, the key step in the prediction is to conduct a short-term creep experiment on bamboo scrimber under relatively high stress levels. In this study, the creep behaviour was compressive. According to a previous study, for this type of creep research, when the experimental stress level reaches 60 % of the compressive strength of the material, the specimen usually breaks within 2 h, which is not beneficial for further analysis [13]. Therefore, in this study, the stress level during the short-term creep experiment was set to 20 % , 30 % and 40 % of the compressive strength. In addition, to verify the universality of the method proposed in this study, four specimens were used for the experiment. The short-term compressive experiment results are shown in detail in Fig. 7.

As shown in Fig. 7, the short-term compressive creep experiment for each specimen under a selected stress level was performed for 150 min. An examination of the recorded strain curves clearly shows that for each

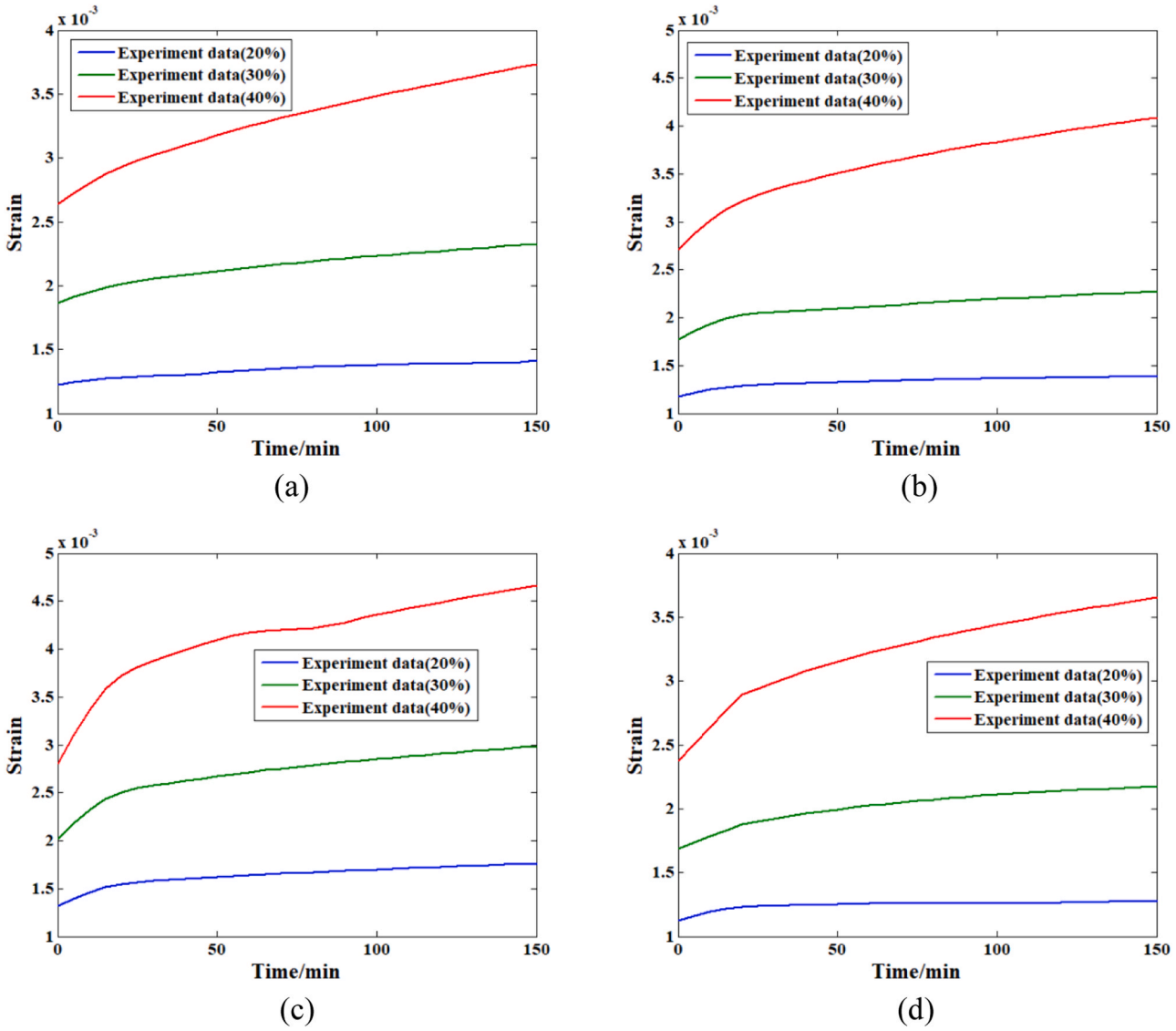


**Fig. 7.** Short-term compressive creep strain histories of the specimen: (a) first specimen; (b) second specimen; (c) third specimen; (d) fourth specimen.

specimen, the slope of the creep strain evolution curve under a lower stress level (20 % of the compressive strength) is lower than that of the same curve under higher stress levels (30 % and 40 % of the compressive strength), which means that higher stress level will generate faster creep strain growth. In addition, the compressive strain growth speed shows small fluctuations, particularly for the experimental results of the third specimen under the stress level of 40 % of the compressive strength. This phenomenon is most likely due to the microstructural features of the specimens. As introduced in Section 2.1, bamboo scrimber is comprised mainly of bamboo fibre and phenolic resin. The creep properties of these two materials are quite different, resulting in an uneven distribution of defects among the inner parts of the specimen when the load is applied. In addition, the pores between these components may be destroyed with increasing the accumulated damage. This accelerates the evolution process to some degree.

For a more comprehensive comparison of the creep results, a normalization method is chosen to analyse the strain history. In accordance with the American standard ASTM D6815—09, the definition of relative creep can be expressed as follows:

$$\xi(t) = \frac{\varepsilon(t)}{\varepsilon(t=0)} \tag{25}$$

Fig. 8 shows the detailed information of this parameter obtained from all four samples under all four stress levels, from which it can be found that the relative creep of the sample is obviously influenced by the stress applied to it. For all four samples, the relative creep steadily increases with increasing stress. The detailed information of the creep experiment results were shown in Table 2.

### 3.3. Model analysis results

Based on the experimental data obtained in the previous section and the variable-order Caputo fractional derivative-defined Maxwell model, it was possible to analyse the viscoelastic mechanical properties of the specimen under the corresponding load conditions. The fitting results are shown in Fig. 8.

As shown in Fig. 8, for all four specimens under the selected stress levels, the fitting results based on the proposed Maxwell model were quite close to the experimental data. The accuracy of the fitting results may be lower at some points in time within the initial stage; however, the relative accuracy throughout the creep process was still sufficiently high. Table 2 presents detailed information on the model parameters obtained from the fitting process, showing that the values of all correlation coefficients are greater than 98 %, which means that the accuracy

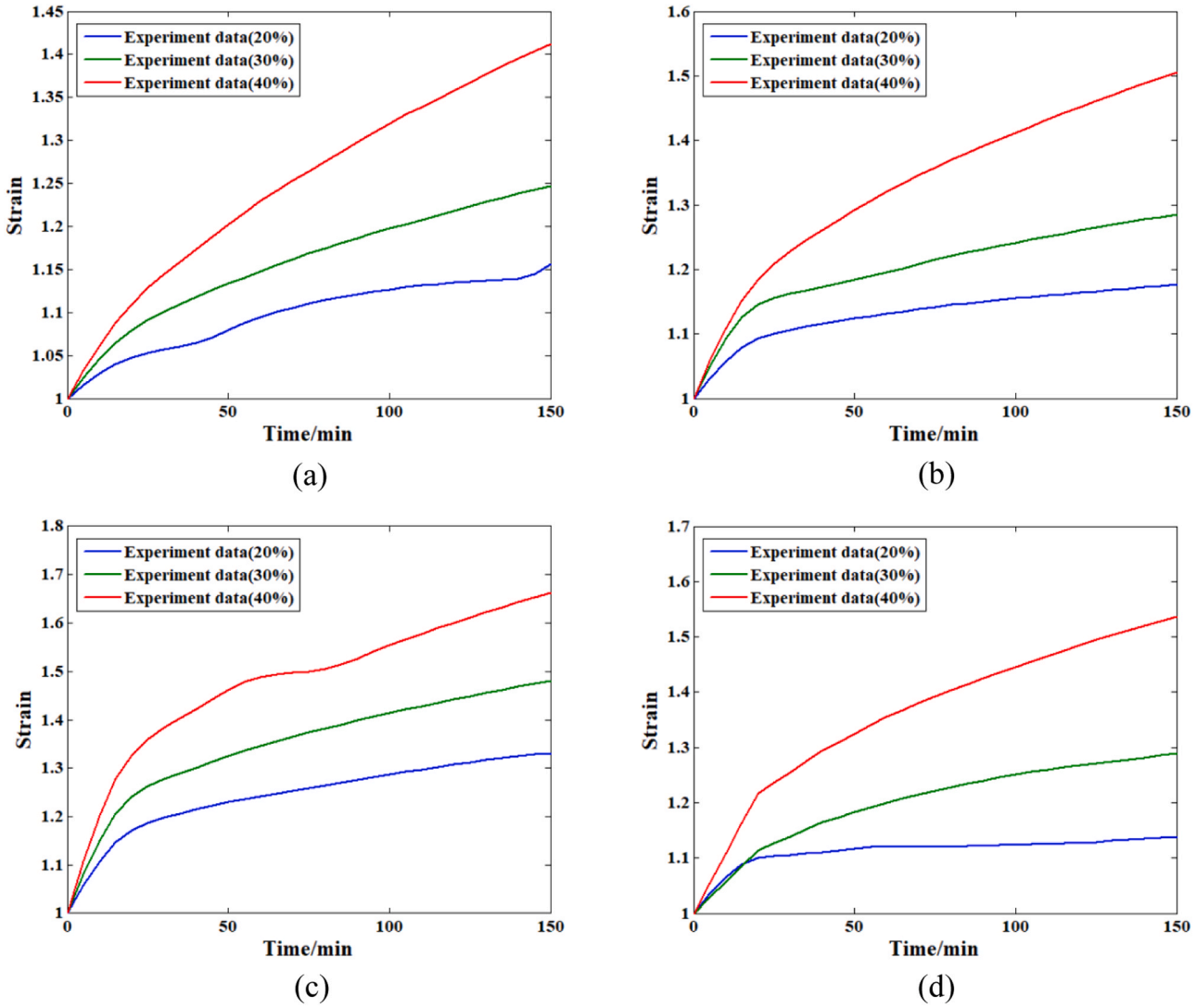


**Fig. 8.** Relative creep analysis of the samples under different stress levels: (a) first sample, (b) second sample, (c) third sample, and (d) fourth sample.

**Table 2**
The statistical analysis results of the creep experiment data.

| Specimen number | Stress level | Initial strain | Final strain | Growth rate |
|---|---|---|---|---|
| 1 | 40 % | 0.002642 | 0.003728 | 41.1 % |
| | 30 % | 0.001865 | 0.002326 | 24.7 % |
| | 20 % | 0.001224 | 0.001415 | 15.6 % |
| 2 | 40 % | 0.002715 | 0.004089 | 50.6 % |
| | 30 % | 0.001768 | 0.002272 | 28.5 % |
| | 20 % | 0.00118 | 0.001389 | 17.7 % |
| 3 | 40 % | 0.002803 | 0.004661 | 66.3 % |
| | 30 % | 0.002017 | 0.002995 | 48.5 % |
| | 20 % | 0.00132 | 0.00176 | 33.3 % |
| 4 | 40 % | 0.002378 | 0.003652 | 53.6 % |
| | 30 % | 0.001687 | 0.002241 | 32.8 % |
| | 20 % | 0.001121 | 0.001276 | 13.8 % |

of the fitting results is sufficiently high for engineering applications. However, the parameter values obtained from different specimens were quite different, even though the same stress level was applied in the creep experiment. This result can be explained by the mechanical property variation of the material itself. According to the manufacturing process of the recombinant bamboo, this natural fiber reinforced composite material is manufactured through the pressing technology, which may result in the inhomogeneous distribution of the fiber and the phenolic resin within the specimen, as well as the polytropy of the mechanical property [24].

On the other hand, from the fitting results of all the four specimens, it's obvious that when the higher stress level (40 % of the compressive strength) is applied on a specimen, the value of the order will also be larger. While for the viscosity coefficient, the situation is completely the opposite. According to the theory of fractional order, this phenomenon means that the material has more obvious rheological properties under the relatively higher stress level, which is in accordance with the creep increase speed.

### 3.4. Prediction results

The compressive creep strain growth process of a specimen under different stress levels can be predicted based on the model parameters obtained through the fitting process. In addition, according to the fitting results in Table 2, the stress level of the experiment affects the values of both the order and viscosity coefficients. Therefore, the determination of the values of the parameters at the given stress level is a key step in predicting the compressive creep strain under other stress levels. In this study, combinations of two types of commonly used functions were used to calculate the parameter values under other stress levels. Detailed information regarding these combinations is presented in Table 3.

As shown in Table 3, the power and exponential functions were

**Table 3**
Model parameters obtained from the fitting.

| Specimen number | 20 % stress level | 30 % stress level | 40 % stress level |
|---|---|---|---|
| 1 | $E_0 = 12.1GPa$<br>$\eta_0 = 1234GPa{\cdot}min^{-1}$<br>$\alpha = 0.4872$<br>$R^2 = 0.9879$<br>$RMSE = 0.0131$ | $E_0 = 12.2GPa$<br>$\eta_0 = 994GPa{\cdot}min^{-1}$<br>$\alpha = 0.5467$<br>$R^2 = 0.9951$<br>$RMSE = 0.0058$ | $E_0 = 11.5GPa$<br>$\eta_0 = 796GPa{\cdot}min^{-1}$<br>$\alpha = 0.6199$<br>$R^2 = 0.9962$<br>$RMSE = 0.0038$ |
| 2 | $E_0 = 11.4GPa$<br>$\eta_0 = 556GPa{\cdot}min^{-1}$<br>$\alpha = 0.352$<br>$R^2 = 0.9963$<br>$RMSE = 0.0046$ | $E_0 = 11.8GPa$<br>$\eta_0 = 468GPa{\cdot}min^{-1}$<br>$\alpha = 0.4167$<br>$R^2 = 0.9924$<br>$RMSE = 0.0076$ | $E_0 = 11.2GPa$<br>$\eta_0 = 356GPa{\cdot}min^{-1}$<br>$\alpha = 0.499$<br>$R^2 = 0.9981$<br>$RMSE = 0.0082$ |
| 3 | $E_0 = 10.9GPa$<br>$\eta_0 = 241GPa{\cdot}min^{-1}$<br>$\alpha = 0.325$<br>$R^2 = 0.9972$<br>$RMSE = 0.0046$ | $E_0 = 10.8GPa$<br>$\eta_0 = 196GPa{\cdot}min^{-1}$<br>$\alpha = 0.37$<br>$R^2 = 0.9966$<br>$RMSE = 0.0142$ | $E_0 = 11.2GPa$<br>$\eta_0 = 182GPa{\cdot}min^{-1}$<br>$\alpha = 0.404$<br>$R^2 = 0.9877$<br>$RMSE = 0.0121$ |
| 4 | $E_0 = 13.1GPa$<br>$\eta_0 = 539GPa{\cdot}min^{-1}$<br>$\alpha = 0.308$<br>$R^2 = 0.9858$<br>$RMSE = 0.0211$ | $E_0 = 13.5GPa$<br>$\eta_0 = 364GPa{\cdot}min^{-1}$<br>$\alpha = 0.3723$<br>$R^2 = 0.9988$<br>$RMSE = 0.0156$ | $E_0 = 12.8GPa$<br>$\eta_0 = 292GPa{\cdot}min^{-1}$<br>$\alpha = 0.448$<br>$R^2 = 0.9989$<br>$RMSE = 0.0169$ |

**Table 4**
Different combinations of functions used to analyse the relationship between the stress level and the main model parameters.

| Serial number of the combination | Order | Viscoelastic coefficient |
|---|---|---|
| 1 | Power function | Power function |
| 2 | Power function | Exponential function |
| 3 | Exponential function | Power function |
| 4 | Exponential function | Exponential function |

arranged in several combinations to analyse the relationship between the stress level and the main model parameters. For the power function, the relationship between the stress level and the model parameter can be expressed as:

$$P = A\sigma^B \tag{26}$$

as shown in Eq. (15), among which $P$is the model parameter, $\sigma$ is the amplitude of the stress level (MPa) applied on the specimen, $A$and $B$are both specimen-calibrated coefficients of the given specimen. While for the exponential function, the definition of the relationship is:

$$P = C\exp(D\sigma) \tag{27}$$

as shown in Eq. (16), $C$ and $D$ are also specimen-calibrated coefficients of the given specimen. According to these two equations, it's not difficult to find out that the values of the function parameters can be easily determined based on the model parameters obtained from the experiments conducted under two different stress levels. The detailed results are shown in Table, 5.

As shown in Table 5, based on these combinations, the values of the model parameters under other stress levels, as well as the predicted values of the creep strain under the same stress level, can be easily calculated. Here, the compressive creep strain growth process of the same four specimens at a relatively low stress level (10 % compressive strength) was selected for the prediction. The values of the main model parameters under this stress level based on different functions are shown in Table 6.

As shown in Table 6, when the values of the main model parameters are calculated based on different functions, the results are also obviously different. In order to comprehensively compare the feasible of the predictions based on different functions, all the combinations in Table 4 are selected in predicting the creep strain growth property under this stress level. The results of the model predictions are presented in Fig.10.

As shown in Fig.10, when the third combination was applied, the predictions of the creep strain evolution process were quite close to the

**Table 5**
The relationship between the stress level and the model parameters.

| Order | | | Viscoelastic coefficient | | |
|---|---|---|---|---|---|
| Specimen number | Power | Exponential | Specimen number | Power | Exponential |
| 1 | $A = 0.1397$<br>$B = 0.4368$ | $C = 0.375$<br>$D = 0.01658$ | 1 | $A = 1.109e+04$<br>$B = -0.7722$ | $C = 1936$<br>$D = -0.02931$ |
| 2 | $A = 0.05885$<br>$B = 0.6265$ | $C = 0.2427$<br>$D = 0.02378$ | 2 | $A = 9127$<br>$B = -0.9508$ | $C = 1063$<br>$D = -0.03609$ |
| 3 | $A = 0.1424$<br>$B = 0.3056$ | $C = 0.2842$<br>$D = 0.0116$ | 3 | $A = 438.3$<br>$B = -0.2576$ | $C = 244.8$<br>$D = -0.009777$ |
| 4 | $A = 0.04988$<br>$B = 0.6434$ | $C = 0.2137$<br>$D = 0.02442$ | 4 | $A = 3986$<br>$B = -0.7661$ | $C = 705.1$<br>$D = -0.02908$ |

**Table 6**
The values of the model parameters based on different functions.

| Order | | | Viscoelastic coefficient | | |
|---|---|---|---|---|---|
| Specimen number | Power | Exponential | Specimen number | Power | Exponential |
| 1 | 0.338 | 0.425 | 1 | $2321GPa \times min^{-1}$ | $1550GPa{\cdot}min^{-1}$ |
| 2 | 0.223 | 0.296 | 2 | $1330GPa{\cdot}min^{-1}$ | $808GPa{\cdot}min^{-1}$ |
| 3 | 0.264 | 0.31 | 3 | $260GPa{\cdot}min^{-1}$ | $227GPa{\cdot}min^{-1}$ |
| 4 | 0.184 | 0.257 | 4 | $845GPa{\cdot}min^{-1}$ | $566GPa{\cdot}min^{-1}$ |

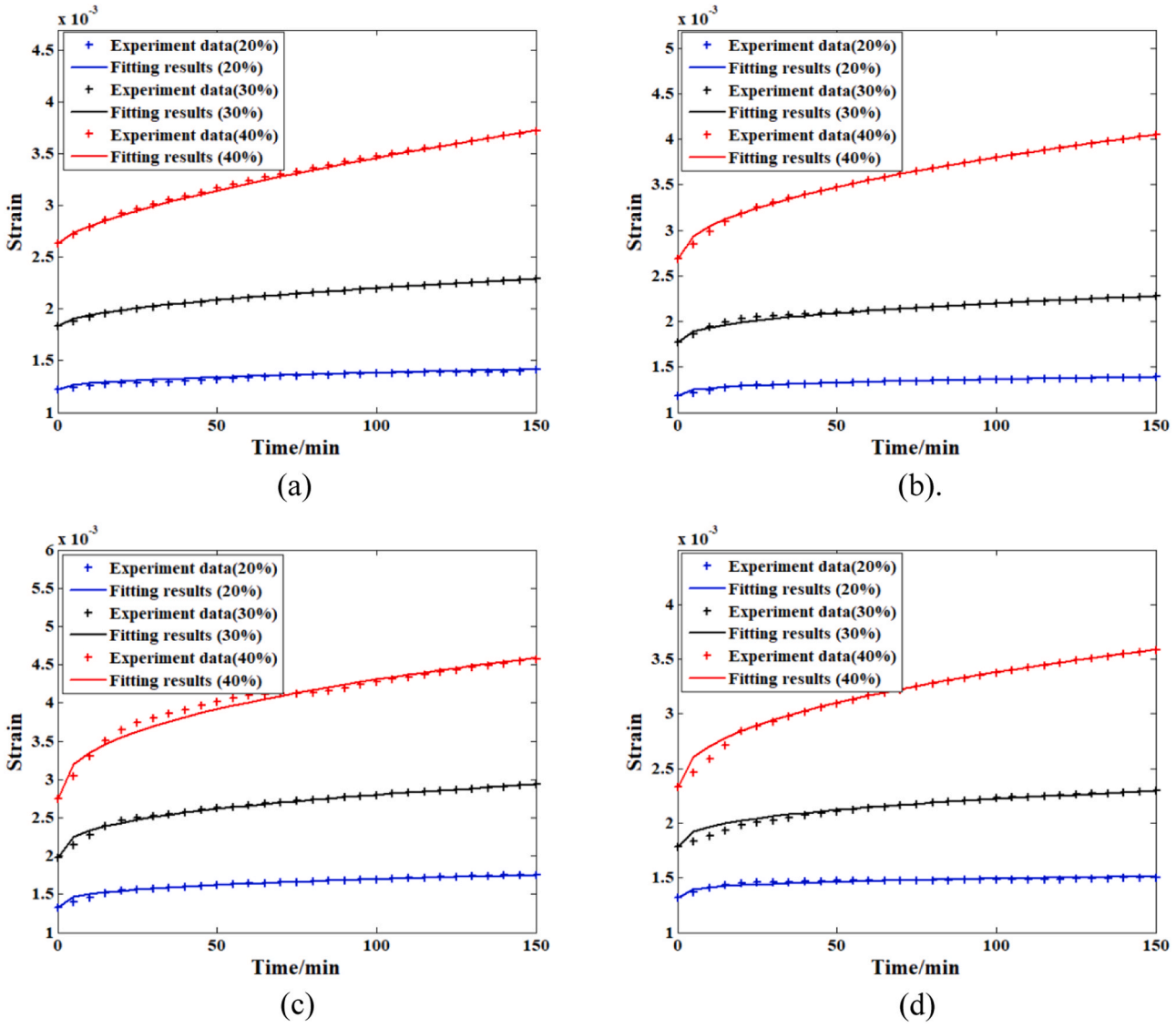


**Fig. 9.** Fitting results of the variable-order Caputo fractional derivative defined Maxwell model for the (a) first specimen; (b) second specimen; (c) third specimen; (d) fourth specimen.

actual experimental data points (the relative difference at any point in time during the experimental process was less than 2 %). Fig.11 shows the detailed information of the residual curves based on this combination [25]. For predictions based on the other three combinations, clear deviations from the experimental data are observed. The prediction and corresponding experimental verification were performed for 600 min. For the short-term compressive creep experiments under three relatively high stress levels, the experimental process was performed for 450 min. Therefore, the prediction can save 25 % of the experimental time and obtain nearly the same experimental results, clearly demonstrating the acceleration of the experimental process achieved by using the model. In addition, although the model parameters obtained from different specimens shows obvious randomness, the parameters for the prediction were determined by the same specimen, in this way the randomness could be taken into consideration in advance, which will not affect the feasible of the proposed model. In other words, the selected third kind of combination can meet the requirement for the prediction accuracy of all the four specimens, which makes it credible for engineering applications.

On the other hand, from the analysis results shown in Table 3, the mechanical property variation of the material is obvious for the recombinant bamboo. As a result of this, it's necessary to analysis the effect of the main model parameter values on the prediction. On the other hand, the elastic modulus of the spring body can be easily determined according to the initial value of the strain at the beginning of the experiment process. Thus the influence of the main model parameters were conducted based on the order and the viscosity coefficient.

Fig. 12 shows the detailed information of the sensitivity analysis results of the main model parameters, among which a clear conclusion can be proposed that the value of the order has a positive effect on the creep strain growth rate. Generally speaking, the larger value of the order, the quicker growth of the creep strain will be generated. While for the viscosity coefficient, the effect is completely the opposite. In addition, compared with the elastic modulus of the dashpot body, the order affects the strain growth speed more obviously within the definition range.

## 4. Conclusion

Creep performance is one of the most important factors for guaranteeing the safety and reliability of composite materials. In this study, an accelerated compressive creep experiment was designed for bamboo

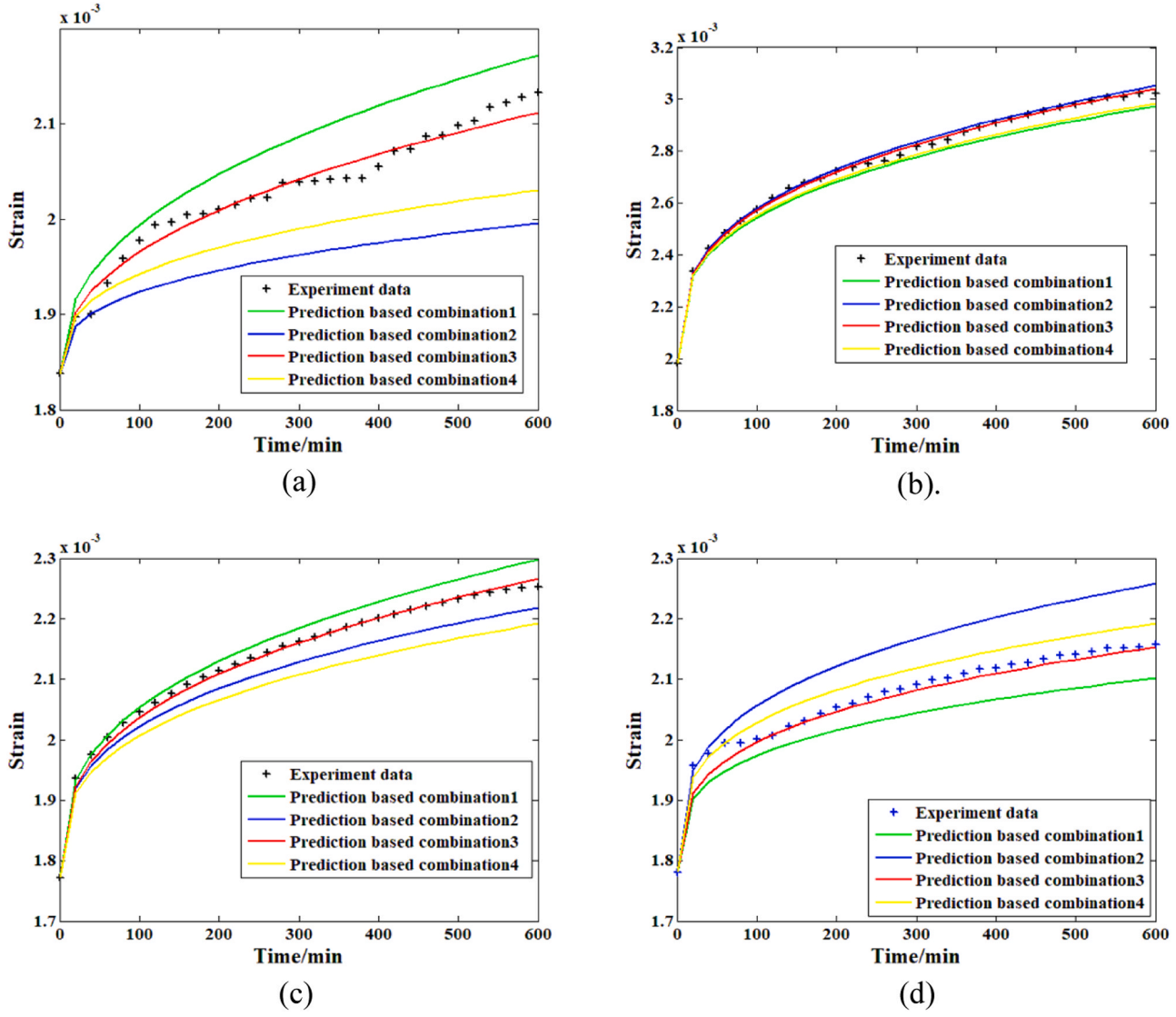


**Fig. 10.** Predicted values of the creep strain under lower stress levels based on different combinations for the (a) first specimen; (b) second specimen; (c) third specimen; and (d) fourth specimen.

scrimber. The key factor of this method is the prediction of the long-term creep strain evolution process under lower stress levels of the bamboo scrimber based on the relatively short-term creep strain evolution process recorded for the same specimen under higher stress levels. The relatively high stress levels were set to 20 %, 30 % and 40 % of the compressive strength of the material. The experimental results under these three load conditions show that the stress level affects the corresponding creep strain growth rate, and the microstructural features of the specimens can, in some cases, result in the fluctuation of the strain signals recorded during the experimental process.

The variable-order Caputo fractional derivative Maxwell model proposed in this study can accurately simulate the compressive strain growth process of all four specimens under given stress levels with a correlation coefficient of 98 % or greater for all cases. The values of the main model parameters show strong variations among the different specimens. This phenomenon can be explained by two factors: the stress level applied to the specimen for the experiment and the variation of the material mechanical properties among the specimens.

When the exponential function is selected to analyse the relationship between the stress level and the order of the proposed Maxwell model, and the power function is selected to analyse the relationship between the stress level and the viscosity coefficient of the same model, the predicted values of the compressive strain under relatively lower stress levels are quite close to the experimental results during a longer experimental period, demonstrating that the actual experiment can be replaced by model predictions. Therefore, the experimental time can be reduced by 25 % to obtain nearly the same experimental data, making this method valuable and suitable for wide application in engineering practice.

## CRediT authorship contribution statement

**Sun Songsong:** Writing – review & editing, Writing – original draft, Project administration, Methodology. **Gong Xiaolin:** Writing – review & editing, Methodology, Funding acquisition. **Miao Zhiwei:** Writing – review & editing, Validation.

## Declaration of Competing Interest

The authors declare that they have no known competing financial interests or personal relationships that could have appeared to influence the work reported in this paper.

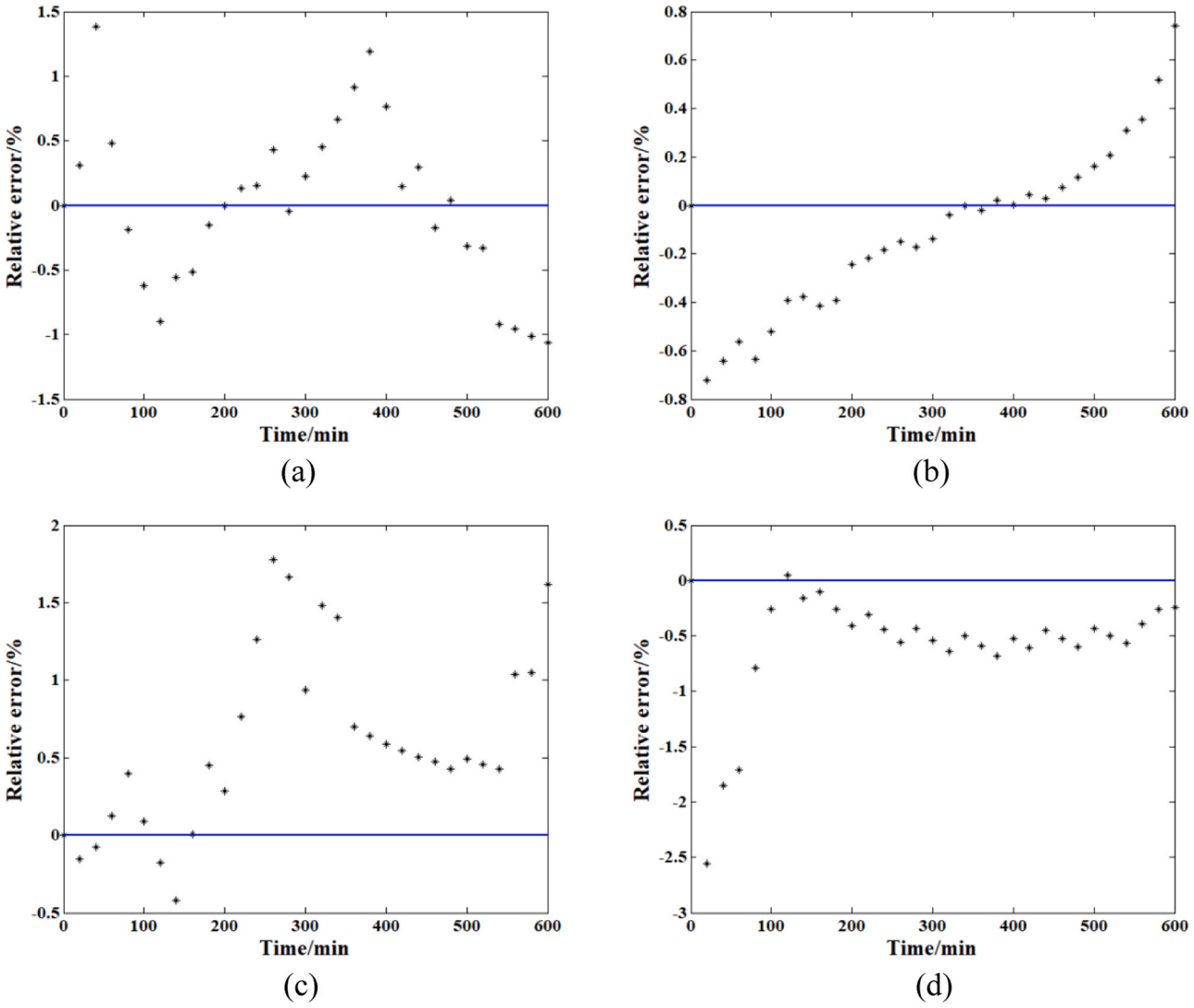


**Fig. 11.** The residual curves of all the four specimens (based on the third combination) (a) first specimen; (b) second specimen; (c) third specimen; and (d) fourth specimen.

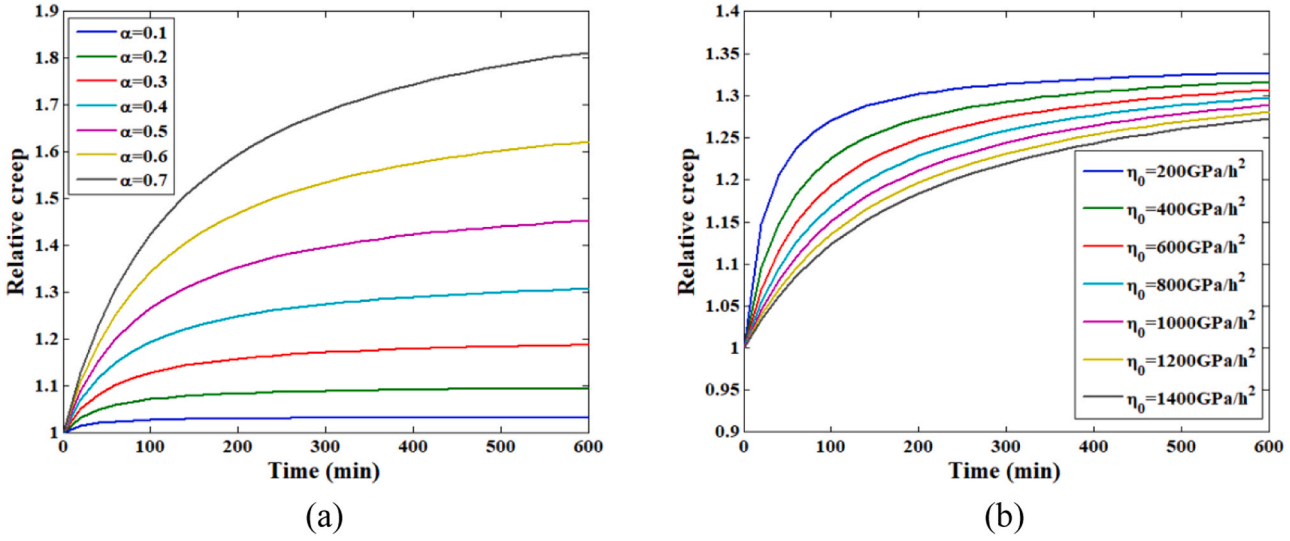


**Fig. 12.** Model parameter sensitivity analysis of the proposed model: (a) results of the order; (b) results of the viscosity coefficient.

## Acknowledgements

This study was supported by the Innovation and Entrepreneurship Training Program of Nanjing Forestry University under Grant Number 202510298089Z, the the Jiangsu Provincial Natural Science Foundation of China under Grant No. BK20200798.

## Appendix

The discretization and analysis of the stress-strain relationship based on the proposed variable-order fractional derivative defined dashpot body is expressed as follows:

$$\begin{aligned}\sigma_2 &= \eta(t)\frac{d^{\alpha}\varepsilon_2(t)}{dt^{\alpha}} \\ &= \eta(t)\int_0^t \frac{\varepsilon_2{}'(\tau)}{\Gamma(1-\alpha)(t-\tau)^{\alpha}}d\tau \\ &\approx \sum_{i=0}^{k}\eta(t_{i+1})\int_{i\mu}^{(i+1)\mu}\frac{\partial\varepsilon_2(\tau)}{\partial\tau}\frac{1}{\Gamma[1-\alpha(t_{i+1})]}\frac{d\tau}{(t_{k+1}-\tau)^{\alpha(t_{i+1})}}\end{aligned} \tag{7}$$

As shown in Eq. (6), $\eta(t_{i+1})$and $\alpha(t_{i+1})$are the viscosity coefficient and order of the Koeller dashpot body in the *ith* time step, respectively, which can be roughly considered as a specimen-calibrated coefficients during this range if the stress level applied on the specimen is unchanged. Based on this assumption, the stress−strain relationship can be expressed as

$$\begin{aligned}\sigma_2 &\approx \sum_{i=0}^{k}\eta(t_{i+1})\frac{\varepsilon_2(t_{i+1})-\varepsilon_2(t_{i+1})}{\mu}\int_{i\mu}^{(i+1)\mu}\frac{1}{\Gamma[1-\alpha(t_{i+1})]}\frac{d\tau}{(t_{k+1}-\tau)^{\alpha(t_{i+1})}} \\ &= \sum_{i=0}^{k}\eta(t_{i+1})\frac{\varepsilon_2(t_{i+1})-\varepsilon_2(t_{i+1})}{\mu}\int_{(k-i)\mu}^{(k-i+1)\mu}\frac{1}{\Gamma[1-\alpha(t_{i+1})]}\frac{d\varphi}{\varphi^{\alpha(t_{i+1})}} \\ &= \sum_{i=0}^{k}\eta(t_{i+1})\frac{\varepsilon_2(t_{i+1})-\varepsilon_2(t_{i+1})}{\mu}\int_{i\mu}^{(i+1)\mu}\frac{1}{\Gamma[1-\alpha(t_{i+1})]}\frac{d\varphi}{\varphi^{\alpha(t_{i+1})}} \\ &= \sum_{i=0}^{k}\eta(t_{i+1})\frac{\varepsilon_2(t_{i+1})-\varepsilon_2(t_{i+1})}{\mu}\frac{1}{\Gamma[1-\alpha(t_{i+1})]}\int_{i\mu}^{(i+1)\mu}\frac{d\varphi}{\varphi^{\alpha(t_{i+1})}} \\ &= \sum_{i=0}^{k}\eta(t_{i+1})[\varepsilon_2(t_{i+1})-\varepsilon_2(t_{i+1})]\frac{\mu^{-\alpha(t_{i+1})}}{\Gamma[2-\alpha(t_{i+1})]}[(i+1)^{1-\alpha(t_{i+1})}-i^{1-\alpha(t_{i+1})}]\end{aligned} \tag{8}$$

where $t=(k+1)\mu$and $t$ are the total load times, and $\mu$ is the length of the time step. Based on this, the response strain of the model under a given stress level can be proposed.

## References

[1] Li Haitao, Xue Xin, Xiong Zhenhua, Ashraf Mahmud, Lorenzo Rodolfo, Shuchi Sarah. Application case of laminated bamboo lumber structure – building of sentai bamboo research center. Sustain Struct 2024;4(1):000043.
[2] Zhang Yongchao, Liu Man, Liu Caimei, Wu Xizhi, Li Yutong, Li Xianjun, et al. Experimental, theoretical and numerical study on the shear stress of adhesive layer in FRP-bamboo scrimber composite beams. Sustain Struct 2024;4(1):000041.
[3] Liu Yang, Liu Kun, Wang Wentao, Fan Linlin, Li Binbin. Progress on the connection performance of steel-engineered bamboo beam-column connections under cyclic loads: a review. Sustain Struct 2024;4(1):000037.
[4] Huang Dongsheng, Sheng Baolu, Shen Yurong, et al. An analytical solution for doublecantilever beam based on elastic-plastic bilinear cohesive law: analysis for mode I fracture of fibrous composites. Eng Fract Mech 2018;193:66–76.
[5] Huang Dongsheng, Bian Yuling, Zhou Aiping, et al. Experimental study on stress–strain relationships and failure mechanisms of parallel strand bamboo made from phyllostachys. Constr Build Mater 2015;77:130–8.
[6] Li Haitao, Zhang Huizhong, Zhenyu Qiu, et al. Mechanical properties and stress strain relationship models for bamboo scrimber. J Renew Mater 2020;8(1):13–27.
[7] Ma Xinxin, Li Hui, Zehui Jiang, et al. Flexural fatigue behavior of bamboo-based products. Holzforschung 2020;74(11):1053–60.
[8] Weiwei Shangguan, Yong Zhong, Xinting Xing, et al. Strength models of bamboo scrimber for compressive properties. J Wood Sci 2015;61(2):120–7.
[9] Yu Yanglun, Huang Yuxiang, Zhang Yahui, et al. The reinforcing mechanism of mechanical properties of bamboo fiber bundle-reinforced composites. Polym Compos 2019;40(4):1463–72.
[10] Song Jian, Surjadi JU, Hu Dayong, et al. Fatigue characterization of structural bamboo materials under flexural bending. Int J Fatigue 2017;100:126–35.
[11] Yuan Zhurun, Wu Xinwu, Wang Xinzhou, et al. Effects of one-step hot oil treatment on the physical, mechanical, and surface properties of bamboo scrimber. Molecules 2020;25(19):4488.
[12] Zhao Kunpeng, Wei Yang, Chen Si, et al. Experimental investigation of the long-term behavior of reconstituted bamboo beams with various loading levels. J Build Eng 2020;36:102107.
[13] Wei Yang, Zhao Kunpeng, Hang Chen, et al. Experimental study on the creep behavior of recombinant bamboo. J Renew Mater 2020;8(3).
[14] Si Chen, Yang Wei, Kunpeng Zhao, et al. Experiment on short-term bending creep performance of bamboo scrimber. J Archit Civ Eng 2021;38(5).
[15] Si Chen, Yang Wei, Kunpeng Zhao, et al. Creep performance and prediction model of bamboo scrimber under compression. Acta Mater Compos Sin 2021;38(3).
[16] Liu Yanyan, Huang Dongsheng, Sheng Baolu. Et,al. Prediction of the long-term flexural behavior of glued laminated bamboo using accelerated creep test. Wood Sci Technol 2023;57(14).
[17] Liu Yanyan, Huang Dongsheng, Sheng Baolu, et al. Accelerated creep testing of tensile properties of glued laminated bamboo. Acta Mater Compos Sin 2024;41(2).
[18] SongSong Sun, MaoSong Wan. Evaluation of the applicability of different viscoelasticity constitutive models in bamboo scrimber short-term tensile creep property research. Sci Eng Compos Mater 2021;28(1):363–71.
[19] GB T1041-2008. Plastics-determination of compressive properties. Beijing: China Standard Press; 2008.
[20] Gavin, H.P. The Levenberg-Marquardt method for nonlinear least squares curve-fitting problems. Department of Civil and Environmental Engineering, Duke University; 2013: p. 1–17.
[21] Yang Wei, Xuewei Ji, Maojun Duan, et al. Model for axial stress-strain relationship of bamboo scrimber. Acta Mater Compos Sin 2018;35(3).
[22] Stan F, Turcanu A-M, Fetecau C. Analysis of viscoelastic behavior of polypropylene/carbon nanotube nanocomposites by instrumented indentation. Polymers 2020;12:2535.

[23] Sun Songsong, Wan Maosong. Statistical analysis of bamboo scrimber tensile mechanical property based on different models and experiments. Multidiscip Model Mater Struct 2021;17(4):728–38.
[24] Rao Fei, Ji Yaohui, Huang Yuxiang, et al. Influence of resin molecular weight on bonding interface, water resistance, and mechanical properties of bamboo scrimber composite. Constr Build Mater 2021;292:123458.
[25] Nguedjio LC, Mabekou, Takam JS, Blaysat B, et al. Formulation and numerical verification of a new rheological model for creep behavior of tropical wood species based on modified variable-order fractional element. Forests 2025;16:824.